

Title	Frontal wedge deformation near the source region of the 2011 Tohoku-Oki earthquake
Author(s)	Ito, Yoshihiro; Tsuji, Takeshi; Osada, Yukihiro; Kido, Motoyuki; Inazu, Daisuke; Hayashi, Yutaka; Tsushima, Hiroaki; Hino, Ryota; Fujimoto, Hiromi
Citation	GEOPHYSICAL RESEARCH LETTERS (2011), 38(15)
Issue Date	2011-08-12
URL	http://hdl.handle.net/2433/163434
Right	©2011. American Geophysical Union.
Type	Journal Article
Textversion	publisher

Frontal wedge deformation near the source region of the 2011 Tohoku-Oki earthquake

Yoshihiro Ito,¹ Takeshi Tsuji,² Yukihito Osada,¹ Motoyuki Kido,¹ Daisuke Inazu,¹ Yutaka Hayashi,³ Hiroaki Tsushima,³ Ryota Hino,¹ and Hiromi Fujimoto¹

Received 8 June 2011; revised 23 June 2011; accepted 28 June 2011; published 12 August 2011.

[1] We report an uplift of 5 m with a horizontal displacement of more than 60 m due to the 2011 Tohoku-Oki earthquake. The uplift was measured by an ocean-bottom pressure gauge installed before the earthquake on a frontal wedge, which formed an uplift system near the Japan Trench. Horizontal displacements of the frontal wedge were measured using local benchmark displacements obtained by acoustic ranging before and after the earthquake. The average displacements at the frontal wedge were 58 m east and 74 m east-southeast. These results strongly suggest a huge coseismic slip beneath the frontal wedge on the plate boundary. The estimated magnitude of the slip along the main fault was 80 m near the trench. Our results suggest that the horizontal and vertical deformations of the frontal wedge due to the slip generated the tremendous tsunami that struck the coastal area of northeastern Japan. **Citation:** Ito, Y., T. Tsuji, Y. Osada, M. Kido, D. Inazu, Y. Hayashi, H. Tsushima, R. Hino, and H. Fujimoto (2011), Frontal wedge deformation near the source region of the 2011 Tohoku-Oki earthquake, *Geophys. Res. Lett.*, 38, L00G05, doi:10.1029/2011GL048355.

1. Introduction

[2] Deformation of the landward slope of a trench due to megathrust earthquakes is a major factor in the generation of the tsunamis that accompany earthquakes involving entire subduction zones. A measurement of the displacement at the seafloor due to the earthquake is necessary to determine appropriate tsunami warnings. The M9 2011 Tohoku-Oki earthquake of 11 March, 2011, killed 25,000 people living near the coast of Tohoku, Japan. Estimates of the total fault slip for the earthquake indicate that the distribution of coseismic slip exceeded 50 m in some places [Simons *et al.*, 2011], with especially large slip (up to ~60 m) at a shallow depth under a frontal wedge near the Japan Trench [Lay *et al.*, 2011]. Ide *et al.* [2011] proposed the occurrence of dynamic overshoot of a compliant hanging wall during the earthquake, in which amplified motion of a hanging wall near the Earth's surface is expected with rupture propagation along the thrust fault. In their proposal, the shear stress is reduced to less than the dynamic friction on the shallow-dipping plate boundary because the greatest slip is strongly concentrated in the shallowest part of the fault near the trench.

[3] The earthquake generated a tremendous tsunami; its height near the coast was more than 10 m. As measured by the cabled seafloor pressure gauges TM1 and TM2, the tsunami had a distinct impulsive crest with a height of 5 m and a pulse width of 3 min (Figure 1). A back-propagation analysis using tsunami travel-time data from offshore cabled pressure gauges and real-time kinematic global positioning system (GPS) buoys [Kato *et al.*, 2005] suggested that the impulsive crest was generated near the trench [Hayashi *et al.*, 2011]. Tsunami observations made using cabled pressure gauges around Japan indicated that a dislocation of 57 m along the plate boundary near the trench was required to generate the observed tsunami waveform [Maeda *et al.*, 2011]. Tanioka and Satake [1996] proposed a tsunami generation mechanism associated with horizontal displacement of the sloping ocean bottom near the trench. Tanioka and Seno [2001] also suggested the effect of a compliant sedimentary wedge on tsunami generation; the effect is related to horizontal displacement of the backstop and upward deformation of a frontal wedge near the trench.

[4] Another possible source of the tremendous tsunami is the activation of a branch fault or splay fault that branches from a main fault [Moore *et al.*, 2007], which has been clearly identified in the Nankai subduction zone. Tsuji *et al.* [2011] demonstrated that branch faults and a related uplift system with a dislocation exceeding 100 m existed before the earthquake within the landward slope of the Japan Trench. The relationship between tsunami generation and the pre-existing uplift system in the 2011 earthquake remains an open question.

[5] Here, we report the vertical and horizontal displacements of the seafloor in the source region of the 2011 Tohoku-Oki earthquake as measured by an ocean-bottom pressure gauge and the migration of ocean-bottom instruments. We propose a fault model near the trench based on these observations.

2. Ocean-Bottom Pressure Observations

[6] An autonomous pressure gauge using a pressure sensor (Paroscientific, Inc.) was used to measure vertical static crustal deformation due to the M9 event. The pressure gauge recorded data continuously for one year, with a logging interval of 30 s. Figure 1a shows the observation sites. The pressure gauge was installed at TJT1 in April 2010 and recovered at the end of March 2011, 14 days after the earthquake.

[7] Figure 2 shows the ocean-bottom pressure time series between April 2010 and March 2011, which includes the M9 event. The pressure-gauge data represent sea-level variations around average depths resulting from the ocean tide component. The gradual pressure increase at a rate of 0.3 hPa/day

¹Department of Geophysics, Tohoku University, Sendai, Japan.

²Department of Civil and Earth Resources Engineering, Kyoto University, Kyoto, Japan.

³Meteorological Research Institute, Japan Meteorological Agency, Tsukuba, Japan.

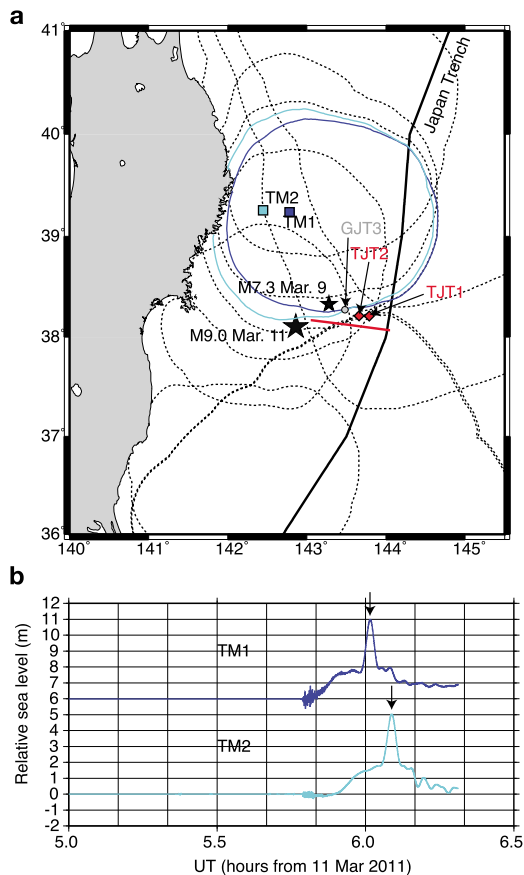


Figure 1. (a) Locations of the observation sites and isotravel time curves of the observed impulsive crest. Red diamonds indicate the offline ocean-bottom observation sites, TJT1 and TJT2. Blue and light blue squares indicate the cabled ocean-bottom pressure gauges, TM1 and TM2, respectively. The isotravel time curves are adapted from *Hayashi et al.* [2011]. Blue and light blue curves indicate isotravel time curves of the impulsive crest observed at TM1 and TM2, respectively. Other dotted curves are isotravel time curves observed at other observation sites such as GPS buoys and other cabled pressure gauges. Large and small stars indicate the hypocenters of the 2011 Tohoku-Oki earthquake and the M7.3 foreshock. The red line indicates the seismic survey line shown in Figure 3d. (b) Tsunami observations by cabled ocean-bottom pressure gauges at TM1 and TM2. Arrows indicate the peaks of the impulsive crest.

arose from the typical instrumental drift seen in ocean-bottom pressure measurements using quartz crystal pressure sensors rather than from geophysical ocean-bottom pressure changes [Watts and Kontoyiannis, 1990]. The diurnal and semidiurnal ocean tides were precisely calculated using harmonic analysis (BAYTAP-G [Tamura et al., 1991]) and were removed from the original data. A large disturbance appears after the earthquake (11 March, 2011, 5:46 UT). The initial disturbance includes a temporary pressure change caused by strong ground motion induced by the seismic wave in the water column. A large negative offset of approximately 500 ± 50 hPa appears clearly after the M9 event. Negative pressure changes represent uplift at the observation points. A change in pressure of 1 hPa

corresponds to roughly 10 mm of vertical displacement; thus, the calculated uplift was 5 ± 0.5 m.

3. Horizontal Displacement of the Frontal Wedge

[8] Two autonomous ocean-bottom seismometers and one pressure gauge with an acoustic release transponder (enabling pop-up release) were installed on the frontal wedge before the earthquake at TJT1 and TJT2, respectively. We measured the locations of the instruments before and after the earthquake at each site to measure the horizontal displacements at TJT1 and TJT2; groups of two and three instruments were used as local benchmarks at TJT1 and TJT2, respectively (see Figure S1a in the auxiliary material).¹

[9] Figures S1b and S1c show the locations of the instruments at TJT1 and TJT2, respectively, calculated before and after the earthquake. The two OBSs at TJT1 moved east, and the three instruments at TJT2 moved east or east-southeast, while roughly maintaining the original geometry of each group of instruments. Note, however, that the acoustic ranging measurement includes a large error of approximately 20 m. This error arose from errors in the measuring ship's position (of ~ 15 m, as determined using a standard GPS instrument, with the antenna located as high above the transducer as possible), limitations on the accuracy of the transponder measurements (~ 1 m), and the uncertainty of actual locations between the GPS antenna and the transducer (~ 5 m).

¹Auxiliary materials are available in the HTML. doi:10.1029/2011GL048355.

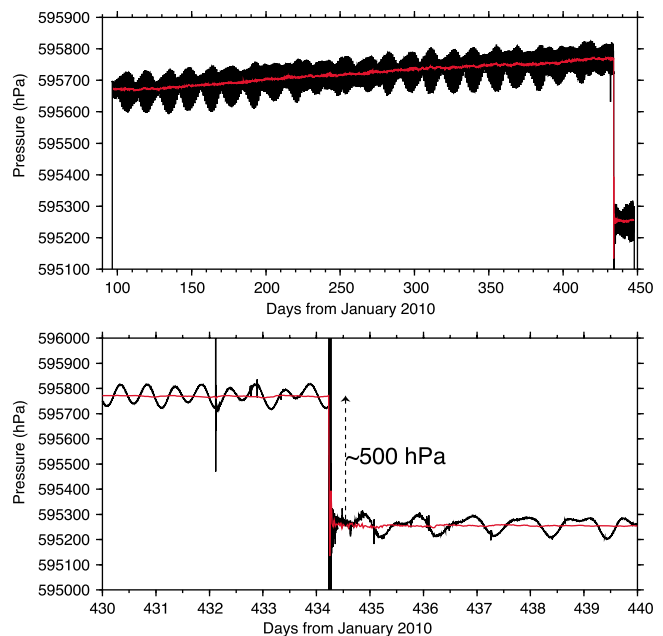


Figure 2. Time series of observed bottom pressures at TJT1. (top) Bottom pressures from April, 2010 to the end of March, 2011. (bottom) Enlargement of the interval between 7 March and 16 March, 2011. Red lines represent observed bottom pressures after the removal of ocean tide effects. Relative variations in pressure (hPa) correspond to relative vertical displacements (cm).

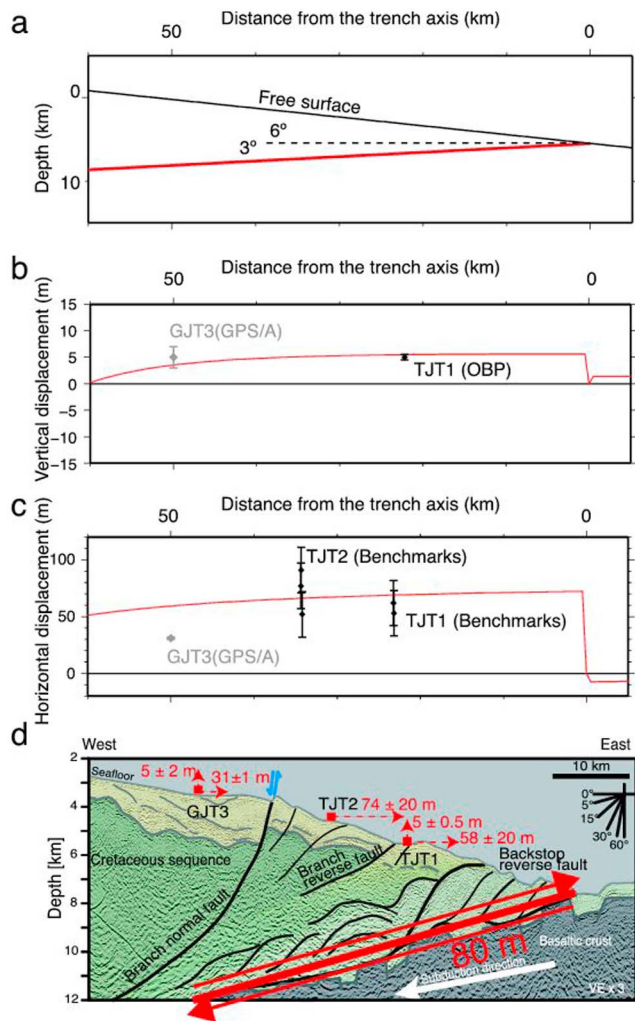


Figure 3. (a) Two-dimensional fault model in the cross-section perpendicular to the trench axis. The red line indicates the plate boundary assumed in a two-dimensional elastic half-space, where the geometry of the plate boundary is taken from seismic reflection and refraction images [Tsuji et al., 2011]. The surface of the elastic half-space dips 6° seaward because of the steep bathymetry around the observation sites. (b) Comparison between observed and predicted vertical displacements. (c) Comparison between observed and predicted horizontal displacements. Diamonds indicate the observed displacement; red curves indicate predicted displacements. Error bars around the diamonds indicate the observation error. The predicted displacement was derived from a fitted fault model with slip magnitudes of 80 m, where the updip end of the suitable fault reached the surface. (d) Pre-existing seismic structure and observed deformation of the frontal wedge. The seismic structure is modified from Tsuji et al. [2011]. Red arrows indicated the observed displacements at TJT1, TJT2, and GJT3. The red line indicates the fault model estimated in this study.

[10] The average displacements at the two sites were 58 m and 74 m, respectively. At TJT1, where an uplift of 5 m was measured by the pressure gauge, two instruments were displaced by 62 ± 20 and 53 ± 20 m, respectively; the

average displacement was 58 m to the east. The location of the gauge at TJT1 after the earthquake was not measured because the gauge was recovered immediately after the earthquake. At TJT2, the three instruments were displaced by 52 ± 20 , 78 ± 20 and 91 ± 20 m, respectively. The gauge at TJT2 could not be recovered, likely due to trouble with the release mechanism.

4. Fault Model

[11] We used a dislocation model in a two-dimensional elastic half-space to fit the observed vertical and horizontal displacements. We assumed the plate boundary to be a fault plane; the assumed geometry of the upper surface of the subducting Pacific plate was based on seismic survey data [Tsuji et al., 2011]. The vertical and horizontal displacements were calculated for a fault model using the dislocation source solution presented by Okada [1992]. The surface of the elastic half-space dips seaward because of the steep bathymetry around the observation sites (Figure 3a).

[12] A suitable model for fitting all of the observations (one vertical displacement and five horizontal displacements) at TJT1 and TJT2 was constructed using a grid-search estimation. By varying the slip magnitude and the distance of the updip end of the fault from the surface along the fault slope, we arrived at a fault model reaching the surface with slip magnitudes of 80 m by minimizing χ^2 (Figures S2 and 3). The downdip limit was fixed at 80 km, where the slope of the upper surface of the subducting plate becomes steeper [Ito et al., 2005]. This is because the observed displacements were limited on the frontal wedge and were insensitive to variation of the downdip limit, although the source models provided by Simons et al. [2011] and Ide et al. [2011] suggest the slippage of a more extensive area exceeding a downdip limit of 100 km. Taking into account the observation errors, the observed horizontal displacements at TJT1 and TJT2 are consistent with those predicted by the model and with the observed uplift at TJT1.

5. Discussion and Conclusions

[13] An uplift of 5 m and a horizontal displacement of 60–70 m were observed at the observation sites TJT1 and TJT2, as predicted by the developed fault model. These sites were located on the frontal wedge of the uplift system proposed by Tsuji et al. [2011], who identified three predominant faults on the basis of the reflection profile before the earthquake. These were (1) a backstop reverse fault, acting as a boundary between the seaward accreted sequence and the landward less-deformed Cretaceous sequence; (2) a branch fault, with reverse faulting composing the seafloor slope break with cold seepage; and (3) a near-vertical normal fault, branching from the plate boundary and extending toward a seafloor ridge (Figure 3d); the seafloor ridge continued parallel to the trench axis for several tens of kilometers. TJT1 was located at the footwall side of the branch fault with reverse faulting. The pressure-gauge data suggest that the branch fault was not activated during the M9 event because the pressure gauge on the footwall would have recorded a subsidence if the branch fault were activated.

[14] A horizontal displacement of more than 20 m was measured just above the epicenter of the 2011 earthquake using a combined GPS/acoustic technique [Sato *et al.*, 2011]. The benchmark for this technique, GJT3, is located landward from the vertical fault with normal faulting; a horizontal displacement of 31 ± 1 m ESE and an uplift of 5 ± 2 m were observed [Kido *et al.*, 2011]. The difference in the observed horizontal displacements at TJT1/TJT2 and GJT3 is 20–40 m, suggesting that an extension regime running ESE–WNW for 20–30 km existed during the earthquake. It is likely that the elongation suggested by the difference in the observed horizontal displacements at the TJT sites and at GJT3 activated the near-vertical normal fault during the earthquake because the large strain of $20\text{--}40\text{ m} / 20\text{--}30\text{ km} \approx 10^{-3}$ was sufficient to break the sedimentary rock beneath the landward slope. Taking into account the observed uplifts at both TJT1 and GJT3, the displacement on the near-vertical normal fault due to the 2011 earthquake was probably less than 1 m.

[15] The simplest fault model that explains the observations is a huge slip of 80 m on the plate boundary beneath the frontal wedge. This huge slip could be interpreted as the effect of the dynamic overshoot proposed by Ide *et al.* [2011]. If the normal fault along the trench axis previously existed between TJT2 and GJT3, this pre-existing weak fault would consequently promote dynamic overshoot because the fault reduces the effective stiffness of the hanging wall. The topography and reflection data show that a displacement along the near-vertical fault branching from the plate boundary has offset a Cretaceous sequence surface by ~ 800 m; a scarp ~ 150 m high marks the trace of the branching fault and exists continuously parallel to the trench axis with a length of several tens of kilometers [Tsuji *et al.*, 2011, Figure 3d]. These geological observations suggest that the near-vertical fault was probably activated by earlier repeated megathrust earthquakes as well as the 2011 earthquake.

[16] The observation sites, TJT1 and TJT2, were located in the source of the tsunami impulsive crest. Figure 1a shows the distribution of the isotravel time curves of the observed impulsive crest. Many isotravel curves converged near sites TJT1 and TJT2, suggesting that the primary source of the impulsive crest was near these sites. The impulsive crest observed at the cabled pressure gauges TM1 and TM2, with a height of 5 m and a pulse width of 3 min (Figure 1b), suggests the deformation of the seafloor around TJT1 and TJT2 in the tsunami source with an uplift of more than 10 m, simply assuming a 1-D tsunami propagation. The observations at TM1 and TM2 also suggest that the tsunami source should have a width of 40 km perpendicular to the trench axis, which was calculated from the tsunami propagation speed, $v = \sqrt{gh}$, and the pulse width of 3 min, where g is the gravitational acceleration constant, and h is the average water depth of 5,000 m on the frontal wedge. The horizontal displacement of the frontal wedge, which has a width of 40 km from the trench axis to the near-vertical normal fault, produced an apparent uplift of 6–7 m by the horizontal displacement effect [Tanioka and Satake, 1996] of the seafloor dipping 6° seaward. The uplift of 11–12 m, including 5 m of uplift due to the coseismic slip on the entire frontal wedge, probably contributed to the generation of the observed impulsive tsunami crest. Our fault model predicts the observed height and pulse width of the impulsive crest and is consistent with the tsunami waveform model by

Maeda *et al.* [2011], in which a fault width of 50 km and a slip of 57 m were assumed beneath our observation sites.

[17] We conclude that the 5 m uplift and 60–70 m displacement of the frontal wedge near the Japan Trench after the 2011 Tohoku–Oki earthquake can be explained by a localized slip of 80 m on the plate boundary near the trench. The observed impulsive tsunami crest may be explained by a horizontal displacement due to dynamic overshoot, which was controlled by the pre-existing fault system within the frontal wedge.

[18] **Acknowledgments.** We thank Greg Moore and an anonymous reviewer for their comments. We also thank Takehi Isse, Aki Ito, and Syuichi Suzuki for their discussion and support onboard the ship and Takashi Furumura and Takuto Maeda for their discussion. This study was supported by MEXT, Japan, under the Observation and Research Program for the Prediction of Earthquakes and Volcanic Eruptions. The study was also supported by JSPS KAKENHI (20244070) and MEXT KAKENHI (21107007). The figures were prepared using the Generic Mapping Tool [Wessel and Smith, 1991].

[19] The Editor wishes to acknowledge Gregory Moore and an anonymous reviewer for their assistance evaluating this paper.

References

- Hayashi, Y., H. Tsushima, K. Hirata, K. Kimura, and K. Maeda (2011), Tsunami source area of the 2011 off the Pacific Coast of Tohoku Earthquake determined from tsunami arrival times at offshore observation stations, *Earth Planets Space*, in press.
- Ide, S., A. Baltary, and G. C. Beroza (2011), Shallow dynamic overshoot and energetic deep rupture in the 2011 M_w 9.0 Tohoku–Oki Earthquake, *Science*, *332*, 1425–1429, doi:10.1126/science.1207020.
- Ito, A., G. Fujie, S. Miura, S. Kodaira, Y. Kaneda, and R. Hino (2005), Bending of the subducting oceanic plate and its implication for rupture propagation of large interplate earthquakes off Miyagi, Japan, in the Japan Trench subduction zone, *Geophys. Res. Lett.*, *32*, L05310, doi:10.1029/2004GL022307.
- Kato, T., Y. Terada, K. Ito, R. Hattori, T. Abe, T. Miyake, S. Koshimura, and T. Nagai (2005), Tsunami due to the 2004 September 5th off the Kii Peninsula earthquake, Japan, recorded by a new GPS buoy, *Earth Planets Space*, *57*, 279–301.
- Kido, M., Y. Osada, H. Fujimoto, R. Hino, and Y. Ito (2011), Huge crustal displacements just above the source region of the Tohoku earthquake observed by GPS/acoustic survey, paper presented at Japan Geoscience Union Meeting, Chiba, Japan.
- Lay, T., C. J. Ammon, H. Kanamori, L. Xue, and M. J. Kim (2011), Possible large near-trench slip during the great 2011 Tohoku (M_w 9.0) earthquake, *Earth Planets Space*, in press.
- Maeda, T., T. Furumura, S. Sakai, and M. Shinohara (2011), Significant tsunami observed at the ocean-bottom pressure gauges at 2011 off the Pacific coast of Tohoku earthquake, *Earth Planets Space*, in press.
- Moore, G. F., N. L. Bangs, A. Taira, S. Kuramoto, E. Pangborn, and H. J. Tobin (2007), Three-dimensional splay fault geometry and implications for tsunami generation, *Science*, *318*, 1128–1131, doi:10.1126/science.1147195.
- Okada, Y. (1992), Internal deformation due to shear and tensile faults in a half-space, *Bull. Seismol. Soc. Am.*, *82*, 1018–1040.
- Sato, M., T. Ishikawa, N. Ujihara, S. Yoshida, M. Fujita, and A. Asada (2011), Displacement above the hypocenter of the 2011 Tohoku–Oki earthquake, *Science*, *332*, 1395, doi:10.1126/science.1207401.
- Simons, M., et al. (2011), The 2011 magnitude 9.0 Tohoku–Oki earthquake: Mosaicking the megathrust from seconds to centuries, *Science*, *332*, 1421–1425, doi:10.1126/science.1206731.
- Tamura, Y., T. Sato, M. Ooe, and M. Ishiguro (1991), A procedure for tidal analysis with a Bayesian information criterion, *Geophys. J. Int.*, *104*, 507–516, doi:10.1111/j.1365-246X.1991.tb05697.x.
- Tanioka, Y., and K. Satake (1996), Tsunami generation by horizontal displacement of ocean bottom, *Geophys. Res. Lett.*, *23*(8), 861–864, doi:10.1029/96GL00736.
- Tanioka, Y., and T. Seno (2001), Sediment effect on tsunami generation of the 1896 Sanriku tsunami earthquake, *Geophys. Res. Lett.*, *28*(17), 3389–3392, doi:10.1029/2001GL013149.
- Tsuji, T., Y. Ito, M. Kido, Y. Osada, H. Fujimoto, J. Ashi, M. Kinoshita, and T. Matsuoka (2011), Potential tsunamigenic faults of the 2011 off the Pacific coast of Tohoku earthquake, *Earth Planets Space*, in press.
- Watts, D. R., and H. Kontoyiannis (1990), Deep-ocean bottom pressure measurement: Drift removal and performance, *J. Atmos. Oceanic Technol.*, *7*, 296–306, doi:10.1175/1520-0426(1990)007<0296:DOBMPD>2.0.CO;2.

Wessel, P., and W. H. F. Smith (1991), Free software helps map and display data, *Eos Trans. AGU*, 72, 441, doi:10.1029/90EO00319.

H. Fujimoto, R. Hino, D. Inazu, Y. Ito, M. Kido, and Y. Osada, Department of Geophysics, Tohoku University, 6-6 Aramaki-aza-aoba, Aoba-ku, Sendai 981-8578, Japan. (yito@aob.gp.tohoku.ac.jp)

Y. Hayashi and H. Tsushima, Meteorological Research Institute, Japan Meteorological Agency, 1-1 Nagamine, Tsukuba, Ibaraki 305-0052, Japan.
T. Tsuji, Department of Civil and Earth Resources Engineering, Kyoto University, Kyotodaigaku-Katsura, Nishikyoku, Kyoto 615-8540, Japan.